Spectrochimica Acta Part A: Molecular and Biomolecular Spectroscopy 137 (2015) 75–89

Contents lists available at ScienceDirect

Spectrochimica Acta Part A: Molecular and Biomolecular Spectroscopy

journal homepage: www.elsevier.com/locate/saa

New metal complexes of N3 tridentate ligand: Synthesis, spectral studies and biological activity

Abbas Ali Salih Al-Hamdani [a], Wail Al Zoubi [b,*]

[a] Department of Chemistry, College of Science for Women University of Baghdad, Baghdad, Iraq
[b] Department of Chemistry, College of Science, University of Damascus, Syria

HIGHLIGHTS

- The thermodynamic parameters, such as ΔE^*, ΔH^*, ΔS^* ΔG^* and K are calculated from the TGA curve using Coats–Redfern method of complex.
- Hyper Chem-8 program has been used to predict structural geometries of compounds in gas phase.
- The synthesized ligand and its metal complexes were screened for their biological activity against bacterial species, two Gram positive bacteria (*Bacillus subtilis* and *Staphylococcus aureus*) and two Gram negative bacteria (*Escherichia coli* and *Pseudomonas aeruginosa*).

GRAPHICAL ABSTRACT

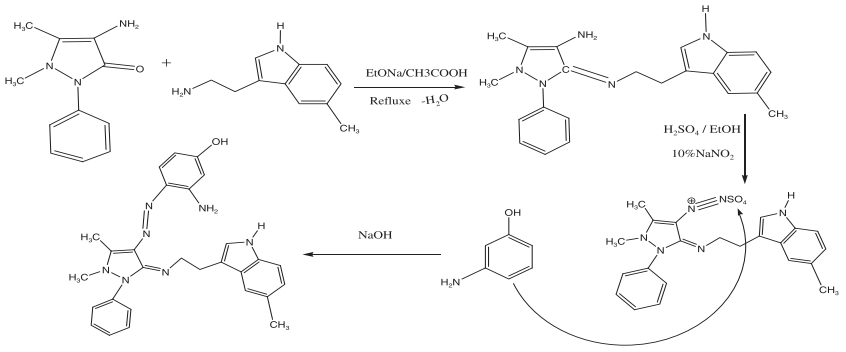

ARTICLE INFO

Article history:
Received 14 May 2014
Received in revised form 2 July 2014
Accepted 18 July 2014
Available online 27 July 2014

Keywords:
Tryptamine
Azo-Schiff base
Spectral studies
Biological activity

ABSTRACT

New tridentate ligand 3-amino-4-{1,5-dimethyl-3-[2-(5-methyl-1H-indol-3-yl)-ethylimino]-2phenyl-2,3-dihydro-1H-pyrazol-4-ylazo}-phenol L was synthesized from the reaction of 1,5-dimethyl-3-[2-(5-methyl-1H-indol-3-yl)-ethylimino]-2-phenyl-2,3-dihydro-1H-pyrazol-4-ylamine and 3.4-amino phenol. A complexes of these ligand $[Ni(II)(L)(H_2O)_2]Cl]Cl$, $[pt(IV)(L)Cl_3]Cl$ and $[M(II)(L)Cl]Cl$ (M = Pd (II), Zn (II), Cd (II) and Hg (II) were synthesized. The complexes were characterized by spectroscopic methods and magnetic moment measurements, elemental analysis, metal content, Chloride containing and conductance. These studies revealed octahedral geometries for the Ni (II), pt (IV) complexes, square planar for Pd (II) complex and tetrahedral for the Zn (II), Cd(II) and Hg (II) complexes. The study of complexes formation via molar ratio and job method in DMF solution has been investigated and results were consistent to those found in the solid complexes with a ratio of (M:L) as (1:1). The thermodynamic parameters, such as ΔE^*, ΔH^*, ΔS^* ΔG^* and K are calculated from the TGA curve using Coats–Redfern method. Hyper Chem-8 program has been used to predict structural geometries of compounds in gas phase. The synthesized ligand and its metal complexes were screened for their biological activity against bacterial species, two Gram positive bacteria (*Bacillus subtilis* and *Staphylococcus aureus*) and two Gram negative bacteria (*Escherichia coli* and *Pseudomonas aeruginosa*).

Introduction

The azo group possesses excellent donor properties and is important in coordination chemistry [1,2], and some azo compounds have been shown to possess good antibacterial activity

* Corresponding author.
E-mail addresses: Abbas_alhamadani@yahoo.co.uk (A.A.S. Al-Hamdani), wwailalzoubi@yahoo.com (W. Al Zoubi).

http://dx.doi.org/10.1016/j.saa.2014.07.057
1386-1425/

[3–8]. Azo Schiff bases are commonly synthesized by coupling a diazonium reagent with an aromatic aldehyde to form an azo aldehyde [9,10]. The azomethine group has good donor properties and can form stable complexes with transition metal ions [11–13]. The azo and azomethine groups on azo Schiff base ligand are oriented in such a way that coordination of both groups to a metal ion is not possible, thus, preferential coordination of the azomethine group while the azo group is left free and uncoordinated has been observed [14–17]. We reported herein the synthesis and spectroscopic studies as well as thermal investigation of novel Azo-Schiff based ligand 3-amino-4-{1,5-dimethyl-3-[2-(5-methyl-1H-indol-3-yl)-ethylimino]-2phenyl-2,3-dihydro-1H-pyrazol-4-ylazo}-phenol. ^{13}C–^{1}H NMR spectra were obtained to determine the structure of the ligand. The Ni(II), Pd(II), Pt(IV), Zn(II), Cd(II) and Hg(II) complexes derived from Schiff base were also prepared and their structures were confirmed by elemental analysis, FT-IR spectroscopy, UV–vis spectroscopy, thermogravimetric analysis and magnetic moment measurements.

Experimental

Materials and methods

All chemicals were obtained from commercial sources and were used without further purifications ($PdCl_2$, $NiCl_2{\cdot}6H_2O$, $CdCl_2{\cdot}H_2O$, $HgCl_2$, $ZnCl_2$, $H_2ptCl_6{\cdot}6H_2O$, $NaNO_2$, K_2CO_3 from BDH. 5-Methyltryptamine hydrochloride, 4-aminophenazon *m*-aminophenol, H_2SO_4, and NaOH from Sigma–Aldrich. All solvents: C_2H_5OH, $CHCl_3$, DMSO, and DMF from Merck.

Physical measurements

Elemental analyses (C, H and N) were carried out on a Heraeus instrument (Vario EL). IR spectra were recorded as KBr or CsI discs using a Shimadzu FT-IR-8300 spectrophotometer from 4000 to 250 cm^{-1}. Electronic spectra were measured from 200 to 900 nm for solutions (10^{-3} M) in DMF at 25 °C using a Shimadzu 160 spectrophotometer. Mass spectra were obtained by positive Electron-Impact (EI) and Fast Atom Bombardment (FAB) was recorded on a VG auto spec micromass spectrometer. NMR spectra were measured in DMSO-d6 solution using Brucker AMX400 MHz and Jeol Lambda 400 MHz spectrometers and thermal analysis studies of the ligand and complexes were performed on a Perkin–Elmer Pyris Diamond DTA/TG thermal system under nitrogen atmosphere at a heating rate of 10 °C/min from 25 to 700 °C. Metals were determined using a Shimadzu (A.A) 680 G atomic absorption spectrophotometer. Chloride was determined using potentiometer titration method on a 686-Titro processor-665Dosimat–Metrohm Swiss. Conductivity measurements were made with DMF solutions using a Jenway 4071 digital conductivity meter and room temperature magnetic moments were measured with a magnetic susceptibility balance (Jonson Mattey Catalytic System Division).

Synthesis of the compound 1,5-dimethyl-3-[2-(5-methyl-1H-indol-3-yl)-ethyl imino]-2-phenyl-2,3-dihydro-1H-pyrazol-4-ylamine (A)

An ethanolic solution (15 ml) of 5-methyltryptamine hydrochloride (1.036 g, 0.00492 mol) was added to a mixture containing an ethanolic solution (25 ml) of 4-amino-1,5-dimethyl-2-phenyl-3-pyrazol-5-one (1 g, 0.00492 mol). The reaction mixture was heated on water bath at (40–50 °C for 14 h in presence of K_2CO_3 after the addition of excess of Ethanol (50 ml). The resulting mixture was refluxed under N_2. A white solid was formed and then recrystallized from mixture (water:ethanol) (1:1). The product was dried over anhydrous $CaCl_2$ in vacuum. Yield: 53.76%(0.95 g), mp 177–179 °C. ^{1}H NMR (DMSO-d6, ppm): δ 1.89 (s, =CCH_3), 2.10 (s, arom-CH_3), 3.43 (s, NCH_3), 3.30 (t, NCH_2), 2.74 (t, CCH_2), 7.64–8.08 (m, arom), 12.11 (s, NH), 4.10(s, NH_2). ^{13}C NMR (100.622 MHz, DMSO-d_6): δ 16.39, 18.87, 38.79, 45.6, 58, 98, 100, 110, 111, 118, 123, 127, 129, 130, 140, 146, 151, (MS) *m*/*z* 360, 164, 201.

Synthesis of the ligand 3-amino-4-{1,5-dimethyl-3-[2-(5-methyl-1H-indol-3-yl)-ethylimino]-2phenyl-2,3-dihydro-1H-pyrazol-4-ylazo}-phenol (L)

A mixture solution from H_2SO_4 (18 M, 2 ml), ethanol (10 ml) and distilled water (10 ml), was charged with (A) (0.5 g, 1.39 mmol). An aqueous solution (2 ml) of $NaNO_2$ (0.0144 g, 1 mmol) was added in drops while maintaining the temperature between 0 and 5 °C to the mixture. After that the diazonium sulphate was added respectively with constant stirring to cold ethanolic solution of *m*-aminophenol (0.151 g, 0.00139 mol), and then solution of 1 M NaOH (25 ml) was added to the dark colored mixture. The mixture was stirred for 1 h at 0 °C and acidified with 1 mL of conc. HCl. The brown product formed was suction filtered and recrystallized from ethanol–water (1:1) and dried (Scheme 1). Yield: 66.45% (0.44 g), mp > 390 °C.^{1}H NMR (DMSO-d^6, ppm): 1.89 (s, C—CH_3), 4.10 (s, NH_2), 4.48 (s, O—H phenol), 12.1 (s, N—H), 7.44 (m, $C_{7,11}$-H), 7.85 (m, $C_{9,18,21}$-H), 8.08 (m, $C_{8,10}$-H). ^{13}C NMR (100.622 MHz, DMSO-d^6) δ 16.39, 18.87, 39.36, 45.6, 58, 98, 100, 106, 110, 112, 119, 124, 126, 129, 130, 133, 140, 145, 153, 158, 168, 182, (MS) *m*/*z* 479, 323,160.

General synthesis of the complexes

Ni (II), Cd (II), Zn (II), Hg (II), Pd (II) and Pt (IV) complexes were prepared in a similar manner using the method described by Nejati and Rezvani. Thus, a solution of 4 mmol of metal salts in 10 ml of ethanol was added to an ethanol–chloroform (1:1 v/v) solution containing 4 mmol of Ligand L and was refluxed for 6 h. The obtained solution was left at room temperature. The resulting precipitates were filtered off, and washed with absolute ethanol and then recrystallized from an ethanol–chloroform (1:3 v/v). Elemental analysis data, colors and yields for the complexes are given in Table 1.

Microbiological investigations

The investigated isolates of bacteria were seeded in tubes with nutrient broth (NB). The seeded NB (1 cm^3) was homogenized in the tubes with 9 cm^3 of melted (45 °C) nutrient agar (NA). The homogeneous suspensions were poured into Petri dishes. The discs of filter paper (diameter 4 mm) were ranged on the cool medium. After cooling on the formed solid medium, 2×10^{-5} dm^3 of the investigated compounds were applied using a micropipette. After incubation for 24 h in a thermostat at 25–27 °C, the inhibition (sterile) zone diameters (including disc) were measured and expressed in mm. An inhibition zone diameter over 7 mm indicates that the tested compound is active against the bacteria under investigation. The antibacterial activities of the investigated compounds were tested against *Escherichia coli* and *Pseudomonas aeruginosa* as Gram negative, *Bacillus subtilis* and *Staphylococcus aureus* as Gram positive. The concentration of each solution was 1.0×10^{-3} mol dm^3. Commercial DMSO was employed to dissolve the tested samples.

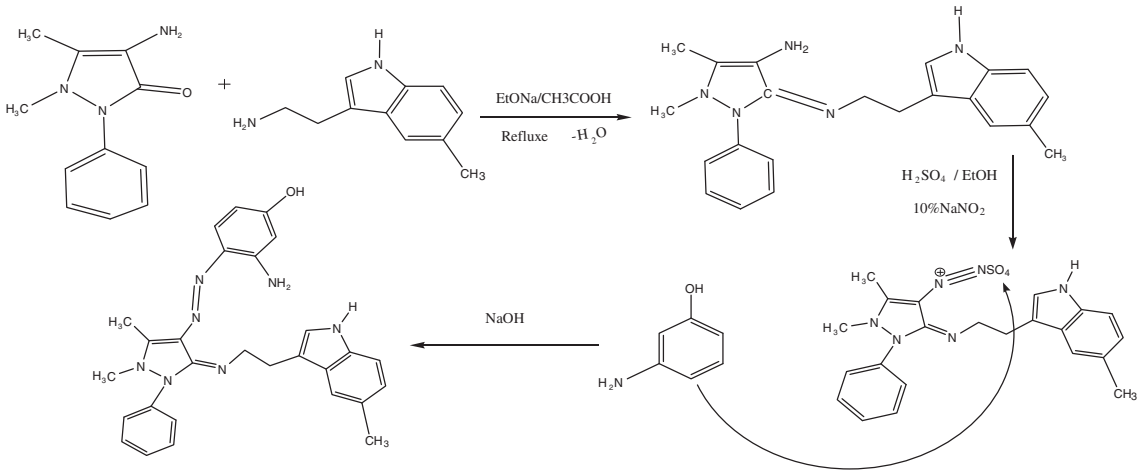

Scheme 1. Synthesis route of ligand.

Table 1
Colours, yields, elemental analyses, and molar conductance values.

Compound	Colour	Yield (%)	Found (Calc.) (%)					Molar conductivity ($cm^2\ \Omega^{-1}\ mol^{-1}$)
			M	C	H	N	Cl	
A	White	73.94		(73.51)	(7.01)	(19.48)		
				75.55	6.87	21.23		
L	Violate	66.45		(70.12)	(6.10)	(20.44)		
	Brown			71.11	6.73	20.08		
$[NiL(H_2O)_2Cl]Cl$	Yellow	68	(9.10)	(52.12)	(5.16)	(15.20)	(10.99)	77
	Green		10.11	51.98	5.87	15.88	9.98 = Cl	
[ZnLCl]Cl	Red	75	(10.62)	(54.61)	(4.75)	(15.92)	(11.51)	77
	Brown		11.08	55.16	4.73	16.28	10.85 = Cl	
[CdLCl]Cl	Red	58	(16.96)	(50.73)	(4.41)	(14.79)	(10.70)	83
	Brown		17.35	51.16	4.11	15.07	11.24 = Cl	
[HgLCl]Cl	Violate	79	(26.71)	(44.78)	(3.89)	(13.05)	(9.44)	70
			27.77	45.97	4.64	13.47	10.06 = Cl	
[PdLCl]Cl	Red	55	(16.20)	(51.19)	(4.45)	(14.93)	(10.79)	77
	Brown		16.74	50.08	4.13	15.33	5.89 = Cl	
$[PtLCl_3]Cl$	Brown	59	(23.89)	(41.19)	(3.58)	(12.01)	(17.37)	77
			24.08	40.00	4.06	13.12	16.42 = Cl	

Programs used in theoretical calculation

Hyper Chem-8 program is a sophisticated molecular modeler, editor and powerful computational package that are known for its quality, flexibility and ease of use. Uniting 2D visualization and animation with quantum chemical calculations, molecular mechanics and dynamic [18]. In the present work, parameterization method 3(PM3) was used for the calculation of heat of formation and binding energy for all metal complexes. PM3 is more popular than other semi-empirical methods due to the availability of algorithms and more accurate than with other methods [19]. PM3/TM is an extension of the PM3 method to include orbital's for use with transition metals. It has parameterized primarily for organic molecules and selected transition metals.

The thermal analysis

From the TGA curves recorded for the successive steps in the decomposition process of these ligand and complexes it was possible to determine the following characteristic thermal parameters for each reaction step: Initial point temperature of decomposition (T_i): the point at which TG curve starts deviating from its base line. Final point temperature of decomposition (T_f): the point at which TG curve returns to its base line. Peak temperature, i.e. temperature of maximum rate of weight loss (T_{DTG}): the point obtained from the intersection of tangents to the peak of TG curve. Mass loss at the decomposition step (Dm): it is the amount of mass that extends from the point T_i up to the reaction end point T_f on the TG curve, i.e. the magnitude of the ordinate of a TG curve. The material released at each step of the decomposition is identified by attributing the mass loss (Dm) at a given step to the component of similar weight calculated from the molecular formula of the investigated complexes, comparing that with literatures of relevant compounds considering their temperature. This may assist identifying the mechanism of reaction in the decomposition steps taking place in the complexes under study. Activation energy (E) of the composition step: the integral method used is the Coats–Redfern equation [20], for reaction order $n \neq 1$or $n = 1$, which when linearized for a correctly chosen n yields the activation energy from the slop;

$$\log\left[\frac{1-1(1-\alpha)^{1-n}}{T^2(1-n)}\right] = \log\frac{ZR}{qE}\left[1-\frac{2RT}{E}\right] - \frac{E}{2.303RT} \quad n = 1$$

$$\log\cdot\left[\frac{-\log\cdot(1-\alpha).}{T^2}\right] = \log\cdot\left[\frac{AR}{\beta E}(1-\frac{2RT}{E}\right] - \frac{E}{2.303RT} \quad \mathrm{n} = 1$$

$\Delta S^* = 2.303R\ [\log(\mathrm{Ah/K}\,T_{\max})]$, $\Delta H^* = E - RT_{\max}$, $\Delta G^* = \Delta H^* - T_{\max}\Delta S^*$. Where α = fraction of weight loss, T = temperature (K), n = order of reaction, A or Z = pre-exponential factor, R = molar gas constant, E = activation energy and q = heating rate. Order of reaction (n): it is the one for which a plot of the Coats–Redfern expression gives the best straight line among various trial values of n that are examined relative to that estimated by the Horovitz–Metzger method [21].

Table 2
IR frequencies (cm^{-1}) of the compounds.

Compound	νas(NH_2) νs(NH_2)	ν(OH) ph ν(CO) ph	ν(NH) δ(NH_2)	ν(C=N)	ν(N=N) + ν(CNNC) ν(C–N=N–C)	ν(M–N)	Additional bands
A	3485 3305	–	3271	1641	–	–	–
L	3439 3330	3530 1307	3115 1604	1670	1446–1407 1115	–	–
[NiL(H_2O)$_2$Cl]Cl	3518 3343	3546 1304	3124 1604	1646	1436–1403 1116	500 470	ν(H_2O) = 3643 δ(H_2O) = 969 ν(Ni–Cl) = 415
[ZnLCl]Cl	3507 3333	3546 1304	3127 1604	1643	1436–1384 1107	536 466	ν(Zn–Cl) = 416
[CdLCl]Cl	3512 3343	3543 1303	3121 1601	1642	1436–1390 1107	536 469	ν(Cd–Cl) = 413
[HgLCl]Cl	3518 3343	3543 1308	3121 1601	1648	1436–1408 1107	536 469	ν(Hg–Cl) = 413
[PdLCl]Cl	3503 3336	3546 1307	3115 1604	1646	1436–1403 1103	530 465	ν(Pd–Cl) = 420
[PtLCl$_3$]Cl	3518 3343	3543 1308	3121 1601	1648	1436–1408 1107	536 469	ν(pt-Cl) = 413

Ph = phenolic, as = asymmetric, s = symmetric.

Table 3
Magnetic moment and UV–vis spectral data in DMF solutions.

Complex	μ_{eff} B.M	λ_{max} (cm^{-1})	λ_{max} (nm)	ε_{max} (L mol^{-1} cm^{-1})	Assignments
A		35,714	280	35,000	$\pi \rightarrow \pi^*$
		33,333	300	36,900	$n \rightarrow \pi^*$
L		36,630	273	36,900	$\pi \rightarrow \pi^*$
		33,333	300	39,800	$n \rightarrow \pi^*$
[ZnLCl]Cl	dia	33,783	296	3450	$\pi \rightarrow \pi^*$
		30,769	325	3500	ML → CT and $n \rightarrow \pi^*$
[CdLCl]Cl	dia	33,670	297	2870	$\pi \rightarrow \pi^*$
		26,246	381	3400	ML → CT and n → π^*
[PdLCl]Cl	dia	12,658	790	370	$^1A_1g \rightarrow {}^1A_2g\ \nu_1$
		20,325	492	350	$^1A_1g \rightarrow {}^1B_1g\ \nu_2$
		24,390	410	2500	M → L(CT)
		26,315	380	2800	$n \rightarrow \pi^*$
[HgLCl]Cl	dia	35,714	280	3510	$\pi \rightarrow \pi^*$
		30,864	324	3960	ML → CT and $n \rightarrow \pi^*$
[NiL(H_2O)$_2$Cl]Cl	2.87	29,411	340	130	$n \rightarrow \pi^*$
		25,380	394	160	M → L(C.T)
		20,408	490	40	$^3A_2g(F) \rightarrow {}^3T_1g(P)\ \nu_3$
		15,384	650	45	$^3A_2g(F) \rightarrow {}^3T_1g(F)\nu_2$
[pt LCl$_3$]Cl	0.98	34,602	289	740	$\pi \rightarrow \pi^*$
		19,801	505	120	$^1A_1g \rightarrow {}^1T_2g\ \nu_2$
		12,658	790	100	$^1A_1g \rightarrow {}^1T_1g\ \nu_1$

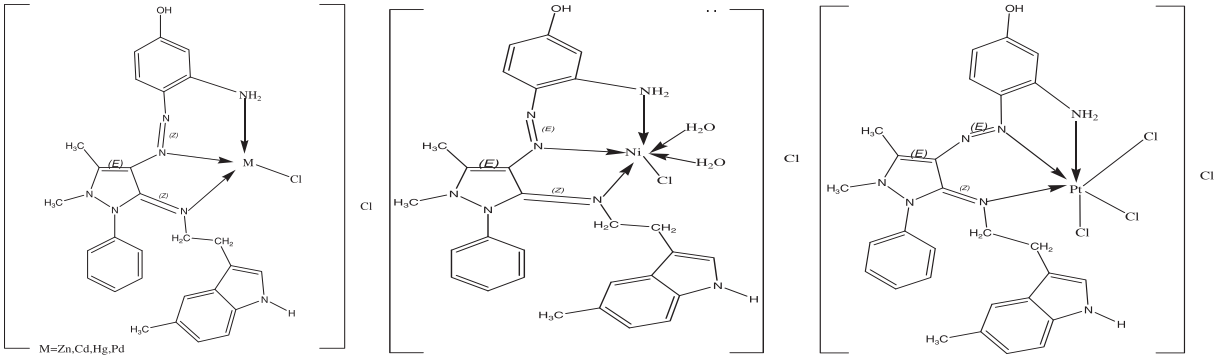

Scheme 2. Proposed structures of metal complexes.

Table 4
Thermal analysis data of some metal complexes of L.

Com	TG range (°C)	DTG_{max} (°C)	% Estimated (calculated)		Assignment
			Mass loss	Total mass loss	
L	32–165 165–383 383–598	77.83 312.17 531.33	13.802 (13.782) 58.094 (58.042) 30.260 (28.385)	102.156 (100.209)	C_5H_6 $C_{17}H_{19}N_4^-$ $C_6H_6N_3O^-$
$[PtLCl_3]Cl$	30–132 132–430 430–700	69.44 314 605.66	5.271(4.342) 22.821(22.842) 50.096(49.676)	78.188 (76.860)	Cl C_3NH_8Cl $C_{25}N_6H_{21}$ PtO
[CdLCl]Cl	30–167 167–700	136.62 570.59	20.282(19.459) 61.015(61.188)	81.297 (80.647)	Cl + C_3H_8N $C_{25}H_{21}N_6$ CdO
[PdLCl]Cl	25–210 210–430 430–698	129.48 305.34 566.05	15.223(15.211) 22.398(21.822) 44.824(44.349)	82.445 (81.382)	C_2H_5 + Cl_2 $C_5H_{13}N_5$ $C_{21}H_{11}N_2$ PdO
[HgLCl]Cl	25–125 125–430 430–698	69.44 314 605.66	5.271(4.72) 22.821(22.460) 43.072(43.995)	71.164 (71.175)	Cl $C_7H_7N_3Cl$ $C_{21}H_{22}N_4$ HgO
$[NiL(H_2O)_2Cl]Cl$	30–158 158–420 420–700	99.66 285.24 597.86	6.127(5.579) 21.601(22.163) 60.994(60.693)	88.722 (88.435)	$2H_2O$ $C_4H_{10}Cl_2N$ $C_{24}H_{19}N_6$ NiO
[ZnLCl]Cl	25–148 148–425 425–695	72.03 359.39 476.91	7.647(8.363) 31.601(32.094) 46.310(46.341)	85.558 (86.798)	Cl + NH_2 $C_5H_{13}N_5$ $C_{21}H_{11}N_2$ ZnO

Table 5
Thermodynamic parameters of the ligand and metal complexes.

Sam (step)	T range (°C)	n	R^2	T_{max} (K)	Ea (kJ mol^{-1})	ΔH^* (kJ mol^{-1})	A Sec^{-1} ×910^7	ΔS^* (J mol^{-1} K^{-1})	ΔG^* (kJ mol^{-1})	$K \times 10^{-7}$
L(1)	32–165	1	0.997	350.98	6.569863	3.6518	2.808	−141.98	53.483	10.96674
L(2)	165–383	1	0.996	582.32	9.029516	4.188	430.8	−104.336	64.945	0.149332
L(3)	383–598	1	0.998	804.45	11.77549	11.7072	967.2	−100.298	92.392	0.100132
CdL = 1	30–167	0.9	0.994	409.77	5.77655	2.37031	1.96163	−107.9613	46.6096	0.11437
CdL = 2	167–700	0.9	0.986	843.74	10.73424	3.71939	18.9976	−95.086	83.9477	0.6349494
HgL1	25–125	0.9	0.998	342.59	5.75888	2.91059	1.48445	−108.79	40.1809	7.47118
HgL = 2	125–430	0.9	0.993	587.15	8.58212	3.70056	4.50492	−104.0388	64.786	0.17224
HgL = 3	430–698	0.9	0.997	878.81	14.05864	6.75222	10.1629	−100.6270	95.1843	0.219906
ZnL = 1	25–148	0.9	0.997	345.18	5.96013	3.09031	1.53688	−108.564	40.5644	7.26656
ZnL = 2	148–425	0.9	0.994	632.54	9.328938	4.07	15.9378	−113.2983	75.7357	5.56647
ZnL = 3	425–695	0.9	0.998	750.06	13.87007	7.63407	6.6931	−102.7828	84.7274	0.12569
NiL = 1	30–158	0.9	0.997	372.81	6.01307	2.91353	1.71005	−108.3165	43.295	8.58393
NiL = 2	158–420	0.9	0.995	558.39	9.016508	4.37405	3.90937	−104.8002	62.8934	0.13074
NiL = 3	420–700	0.9	0.998	871.01	13.5233	6.28172	89.7638	−82.438	78.0861	0.02748
PdL = 1	25–210	0.9	0.995	402.63	9.90618	6.55872	2.60789	−105.4471	49.0149	4.37409
PdL = 2	210–430	0.9	0.996	578.49	9.63113	4.82156	4.18393	−104.5299	65.291	0.127159
PtL = 1	30–132	0.9	0.998	342.59	5.7808	2.9325	2.34722	−104.98	38.8976	0.117239
PtL = 2	132–430	0.9	0.995	587.15	11.19325	6.33296	2.99936	−107.4213	69.4054	6.687478
PtL = 3	430–700	0.9	0.997	878.81	13.6607	6.35428	10.6594	−100.2304	94.4377	0.24356

Results and discussion

The new N3 tridentate ligand L was obtained in good yield by the reaction of 1,5-dimethyl-3-[2-(5-methyl-1H-indol-3-yl)-ethylimino]-2-phenyl-2,3-dihydro-1H-pyrazol-4-ylamine and 3.4-amino phenol, Scheme 1. The ligand was characterized by elemental analysis (Table 1), IR (Table 2), UV–vis (Table 3) respectively. Monomeric complexes of the ligand with Pd(II), Ni(II), pt(IV), Zn(II), Cd(II) and Hg(II) were synthesized by heating 1 mmol of each ligand with 1 mmol of metal chloride, using ethanolic solution. However, in ethanolic, deprotonation of the ligand occur facilitating the formation of the complexes $[Ni(II)(L)(H_2O)_2\ Cl]Cl$, $[pt(IV)(L)Cl_3]Cl$ and [M(II)(L)Cl]Cl (M = Pd(II), Zn(II), Cd(II) and Hg(II)) Scheme 2. The complexes are air-stable solids, soluble in DMF and DMSO, sparingly soluble in MeOH, $CHCl_3$, CH_2Cl_2 and not soluble in other common organic solvents. The analytical data Table 1 agree well with the suggested formulae. The most important infrared bands of the ligand and their complexes together with their assignments are collected in Table 2.

IR spectra

The IR spectrum of the compound A, L and complexes show bands at 3439, 3330 and 1670 cm^{-1} due to the as$\nu(NH_2)$, s$\nu(NH_2)$, $\delta(NH_2)$, and ν(C=N) functional groups, respectively. The ligand show characterization bands at 3530, 1307 and 1446 cm^{-1}due to

Table 6
Antibacterial activity data of ligand and its complexes inhibition zone (mm).

Compound	*Bacillus subtilis* G^+	*Staphylococcus aureus* G^+	*Escherichia coli* G^-	*Pseudomonas aeruginosa* G^-
L	20	17	19	16
$[NiL(H_2O)_2Cl]Cl$	22	20	22	18
[ZnLCl]Cl	24	22	22	22
[CdLCl]Cl	20	22	16	21
[HgLCl]Cl	22	20	22	18
[PdLCl]Cl	24	22	24	22
$[PtLCl_3]Cl$	20	26	16	28

Key to interpretation: less than 10 mm = inactive, 10–15 mm = weakly active, 15–20 mm = moderately active, more than 20 mm = highly active.

Table 7
Comparison of experimental and theoretical vibration frequencies for ligand.

Com	as$\nu(NH_2)$	(NH_2)vs	ν(C=N)	ν(C—N)	ν(N=N)	ν(C=C)	ν(NH)	$\delta(NH_2)$	ν(OH) Phenol	ν(OH) Carboxylic	ν(C—O) Phenol
A	3485*	3305*	1641–1633*	1243*		1591–1556*	3271*	1612*	3699*	3429*	1288*
	3504**	3382**	1867**	1249**		1832**	3452**	1021**	3890**	3885**	1412**
	0***	0***	−0.001***	0***		−0.001***	0***	0.003***	0***	−0.001***	0***
L	3330*	3330*	1670*	1224*	1077*	1550–1496*	3115*	1604*	–	3400*	1203*
	3477**	3405**	1934**	1057**	1911**	1829–1514**	3405**	1206**		3684**	1307**
	0***	0***	−0.001***	0.001***	0.007***	−0.001****	0***	0.001***		0***	0***

the ν(OH) phenolic, ν(C—O) phenolic and ν(N=N), functional groups, respectively. The IR spectra of the complexes exhibited ligand bands with the appropriate shifts due complexes formation Table 2 [22,23].

Moreover, the ν(C=N), ν(N=N), bands of the ligand was observed at 1670, 1446 $cm^{-1}$and this band was shifted to the lower frequencies by (28–22 cm^{-1}) for ν(C=N), and the ν(N=N), bands of the ligand was observed at 1446 $cm^{-1}$and this band was shifted to the lower frequencies by (10 cm^{-1}), in the spectra of the complexes. This indicates that the ligand was coordinated with the metal ions through the N atom. So, it is noted both of the $\nu(NH_2)$ asymmetric and symmetric band of the ligand exhibited at 3439 and 3330 cm^{-1} this band was shifted to the high frequencies by (79–68 cm^{-1}) and (3–13 cm^{-1}) for as$\nu(NH_2)$ and s$\nu(NH_2)$, in the spectra of the complexes. This indicates that the ligand was coordinated with the metal ions through the N atom. The reduction in bond order, upon complexation, can be attributed to delocalization of metal electron density (t_2g) to the π-system of the ligand. These shifts confirm the coordination of the ligand via the nitrogen of azomethine and the azo groups to metal ions.

The ν(NH) band at 3234 cm^{-1}in the free ligand was not shifting for the complexes. At lower frequency the complexes exhibited bands around 536–469 cm^{-1} assigned to the ν(M—N) and exhibited bands around 413–420 cm^{-1} assigned to the ν(M-Cl) for complexes and new bands in $[NiL(H_2O)_2Cl]Cl$ complex the 3643 cm^{-1} and 969 cm^{-1} assigned to the $\nu(H_2O)$ and $\delta(H_2O)$ This indicates that the ligand was coordinated with the Ni(II) ion through the H_2O atom [24,25].

Electronic spectra studies

The electronic spectra of the free ligand L shows electronic transitions $\pi \rightarrow \pi^*$ and $n \rightarrow \pi^*$ at 280 and 300 nm respectively. Finally, the diamagnetic of Zn(II), Cd(II) and Hg(II) complexes exhibited absorption bands at 296, 297 and 280 nm due to $\pi \rightarrow \pi^*$. Appearance of these band are due to $n \rightarrow \pi^*$ transition associated with azomethine linkage and M → L (C.T) charge transfer transition. Moreover, the absorption bands at 296, 297 and 280 nm due to $\pi \rightarrow \pi^*$. Moreover, the spectrum of the complexes also shows bands at 325, 381 and 324 nm due to the charge transfer as the electronic configuration of these complexes Zn (II), Cd (II) and Hg (II) respectively, confirmed the absence of any d-d transition [26,27]. The magnetic moment value 2.75 B.M of Ni(II) complex exhibits peaks at (650 and 490) nm which assign to $^3A_{2g} \rightarrow {}^3T_{1g}(F)$ and $^3A_{2g} \rightarrow {}^3T_{1g}(P)$ transition, respectively suggesting an octahedral geometry around the Ni(II) ion. The magnetic moment value of this complex is consistent with octahedral geometry structure. The spectrum of pt(IV) complex of together with the μ_{eff} value Table 3 exhibits peaks at (790 and 505) nm which assign to $^1A_{1g} \rightarrow {}^1T_{1g}$ and $^1A_{1g} \rightarrow {}^1T_{2g}$ transition, respectively suggest octahedral geometry around pt(VI) complex. The spectrum of Pd(II) complex gave band assigned to $n \rightarrow \pi^*$, M → L (C.T), $^1A_{1g} \rightarrow {}^1B_{1g}$. and $^1A_{1g} \rightarrow {}^1A_{2g}$ (380, 410, 492 and 790) nm respectively suggesting an square planer geometry around the Pd(II) ion. The magnetic moment value of this complex is consistent with square planer geometry [26].

The metal ions complexes discussed herein were dissolved in DMSO and the molar conductivities of their 10^{-3} M solutions at room temperature were measured to establish the charge of the metal complexes. The range of conductance values listed in Table 1 indicates that all the metal complexes have are [1:1] electrolytes [28].

Mass spectrum

Compound (A)

The electron impact spectrum of compound (A) confirms the probable formula by showing a peak at 360 *m/z*, corresponding to Schiff base moiety [($C_{22}H_{25}N_5$), calculated atomic mass 360]. The series of peaks at 164 *m/z* is attributed to $(C_{11}H_{18}N)^+$ and at 201 *m/z* attributed to ($C_{11}H_{13}N_4$). Their intensity gives an idea of the stability of fragments.

Ligand (L)

The electron impact spectrum of the ligand (L) confirms the probable formula by showing a peak at 479 *m/z*, corresponding to Schiff base-Azo moiety [($C_{28}H_{29}N_7O$), calculated atomic mass

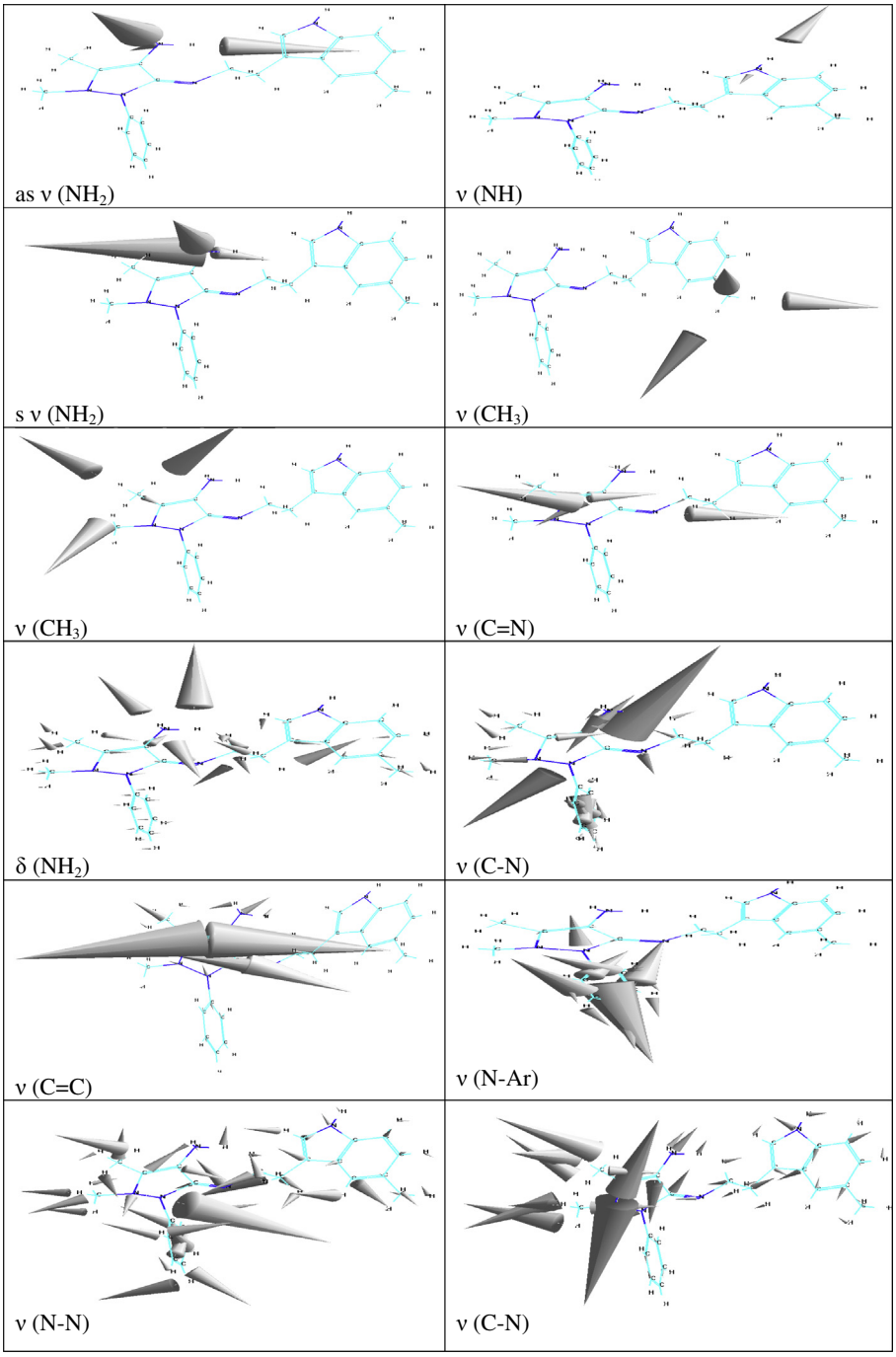

(a)

Fig. 1. The calculated vibrational frequencies of starting material A (a) and ligand L new metal complexes of N3 tridentate ligand: synthesis, spectral (b).

479]. The series of peaks in the range of 323 and 160 *m*/*z* may be assigned to various fragments. Their intensity gives an idea of the stability of fragments.

Complex of ZnL

The electron impact spectrum of [ZnL_2Cl] Cl confirms the probable formula by showing a peak at 615.9 *m*/*z*, corresponding to Complex moiety [($C_{28}H_{29}N_7ZnOCl_2$), calculated atomic mass 615.9]. The series of peaks in the range of 430.3, 429.3, 205.2 and 204.3 *m*/*z* may be assigned to various fragments.

Complex of CdL

The electron impact spectrum of [CdL_2Cl]Cl confirms the probable formula by showing a peak at 662.9 *m*/*z*, corresponding to Complex moiety [($C_{28}H_{29}N_7CdOCl_2$), calculated atomic mass 662.9]. The series of peaks in the range of 430.3, 429.3, 205.2 and 204.3 *m*/*z* may be assigned to various fragments.

Complex of HgL

The electron impact spectrum of [HgL_2Cl]Cl confirms the probable formula by showing a peak at 751 *m*/*z*, corresponding

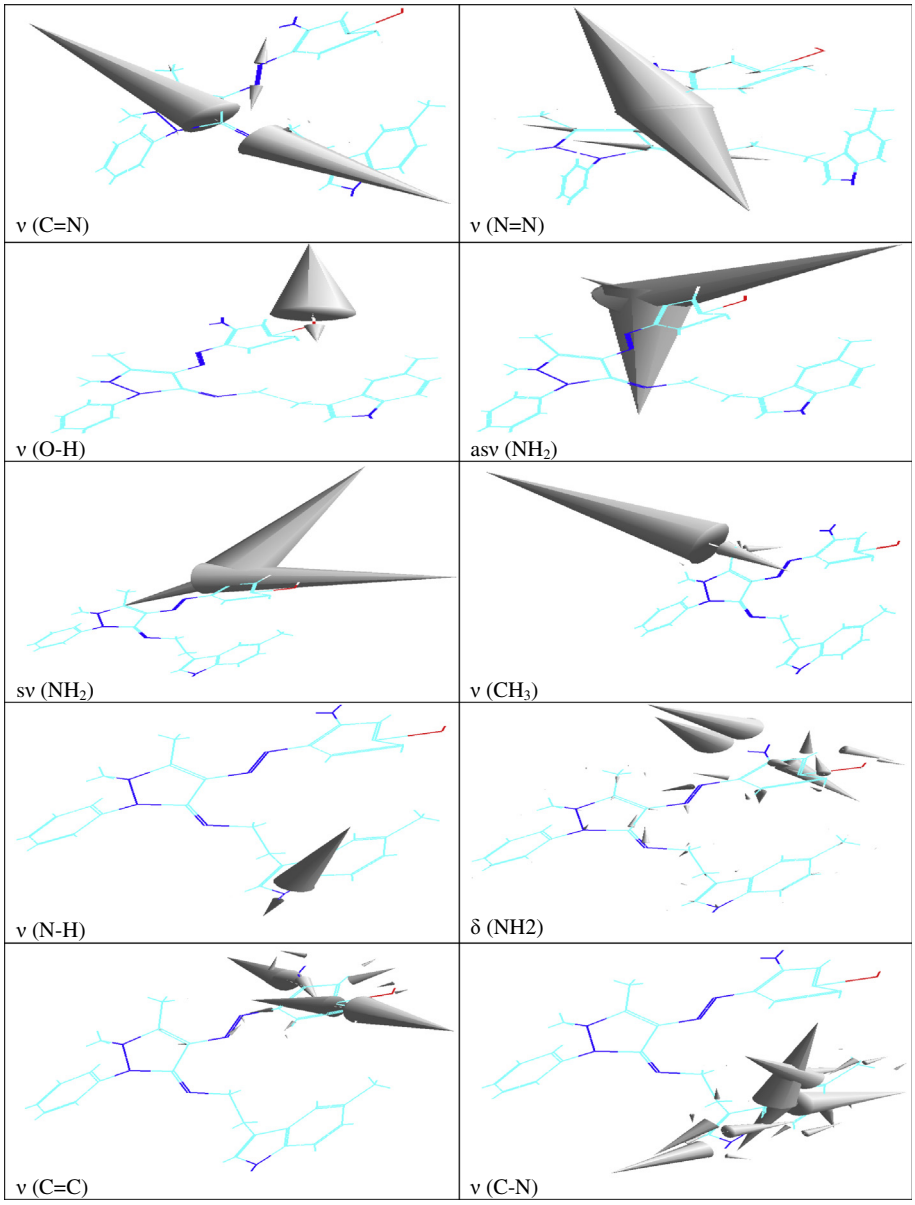

(b)

Fig. 1 (*continued*)

to Complex moiety [($C_{28}H_{29}N_7HgOCl_2$), calculated atomic mass 751]. The series of peaks in the range of 682, 640, 617, 549, 443, 360, 216, 144, 106 and 69 *m*/*z* may be assigned to various fragments.

Complex of PdL

The electron impact spectrum of [PdL_2Cl]Cl confirms the probable formula by showing a peak at 656 *m*/*z*, corresponding to Complex moiety [($C_{28}H_{29}N_7PdOCl_2$), calculated atomic mass 656]. The series of peaks in the range of 369, 354, 296, 287, 208, 128, 125, 122, 88 and 78 *m*/*z* may be assigned to various fragments.

Complex of NiL

The electron impact spectrum of [$NiL_2Cl(H_2O)_2$]Cl confirms the probable formula by showing a peak at 642 *m*/*z*, corresponding to Complex moiety [($C_{28}H_{33}N_7NiO_3Cl_2$), calculated atomic mass 642]. The series of peaks in the range of 369, 354, 276,261,241, 185, 111, 93, 75 and 56 *m*/*z* may be assigned to various fragments.

Complex of PtL

The electron impact spectrum of [ptL_2Cl_3] Cl confirms the probable formula by showing a peak at 816 *m*/*z*, corresponding to Complex moiety [($C_{28}H_{29}N_7PtO_3Cl_4$), calculated atomic mass 816]. The series of peaks in the range of 682, 640, 549, 532, 500, 428, 403, 232, 211, 171, 134, 91 and 72 *m*/*z* may be assigned to various fragments.

Molar ratio

Complex formation by molar ratio of ligand to metal ion was also studied in DMF solution. A series of solutions containing constant concentration of metal ion (1×10^{-3} M) were treated with the same volumes of various concentrations of ligand in presence of potassium hydroxide and heated at 100 °C. The results of L:M titrations were obtained by plotting absorbance of solution mixtures at λ_{max} of the complexes against [L]/[M] which showed a 1:1 M:L ratio for all the complexes, as observed for the solid state

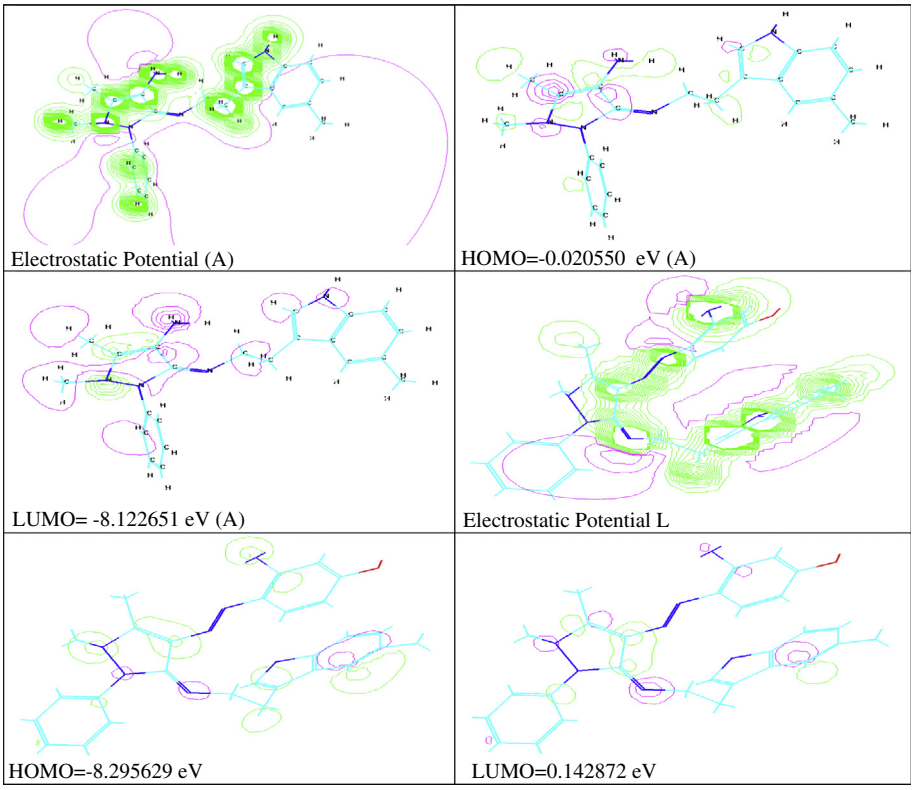

Fig. 2. HOMO and electrostatic potential as for starting material and L.

Table 8
Conformation energetic in (K J Mol^{-1}) for the starting material (A), ligand and complexes.

Com		PM3	AM1
A	Total energy in (0 °K)	−87618.9217849	−96523.8785396
	Total energy in (345.51 °K)	−5430.5535	−5272.7704
	Binding energy	−5484.108206	−5320.1141276
	Heat of formation	143.0217934	307.0158724
	Electronic energy	−761635.0472123	−712416.7481261
	Free energy	−5430.5535	−5272.7704
	Total Dipole moment	3.69133	3.67133
	Zero point energy of vibration	269.87871	268.37399
	Kinetic energy in (345.51 °K)	53.5547	47.3438
L	Total energy in (0 °K)	−119697.7271634	−132546.4762082
	Total energy in (148.73 °K)	−119697.7271634	−132546.4762082
	Binding Energy	−7017.1381464	−6949.6286402
	Heat of formation	129.2988536	196.8083598
	Electronic energy	−1234339.9376185	−1211126.0366310
	Free energy	−119,667	−6890.62
	Total dpole moment	4.44357 Debyes	5.9931Debyes
	Zero point energy of vibration	328.06184	340.12568
	Kinetic energy	28.8175 in (148.73°K)	30.2162 in (155.95 °K)
NiL	Binding energy	−533.2705542	
	Heat of formation	20.3804458	
PdL	Binding energy	−7067.0140643	
	Heat of formation	146.3109357	
ZnL	Binding energy	−6945.1459229	
	Heat of formation	209.3490771	
CdL	Binding energy	−6890.9845825	
	Heat of formation	259.0604175	
HgL	Binding energy	−6945.7550429	
	Heat of formation	192.2599571	

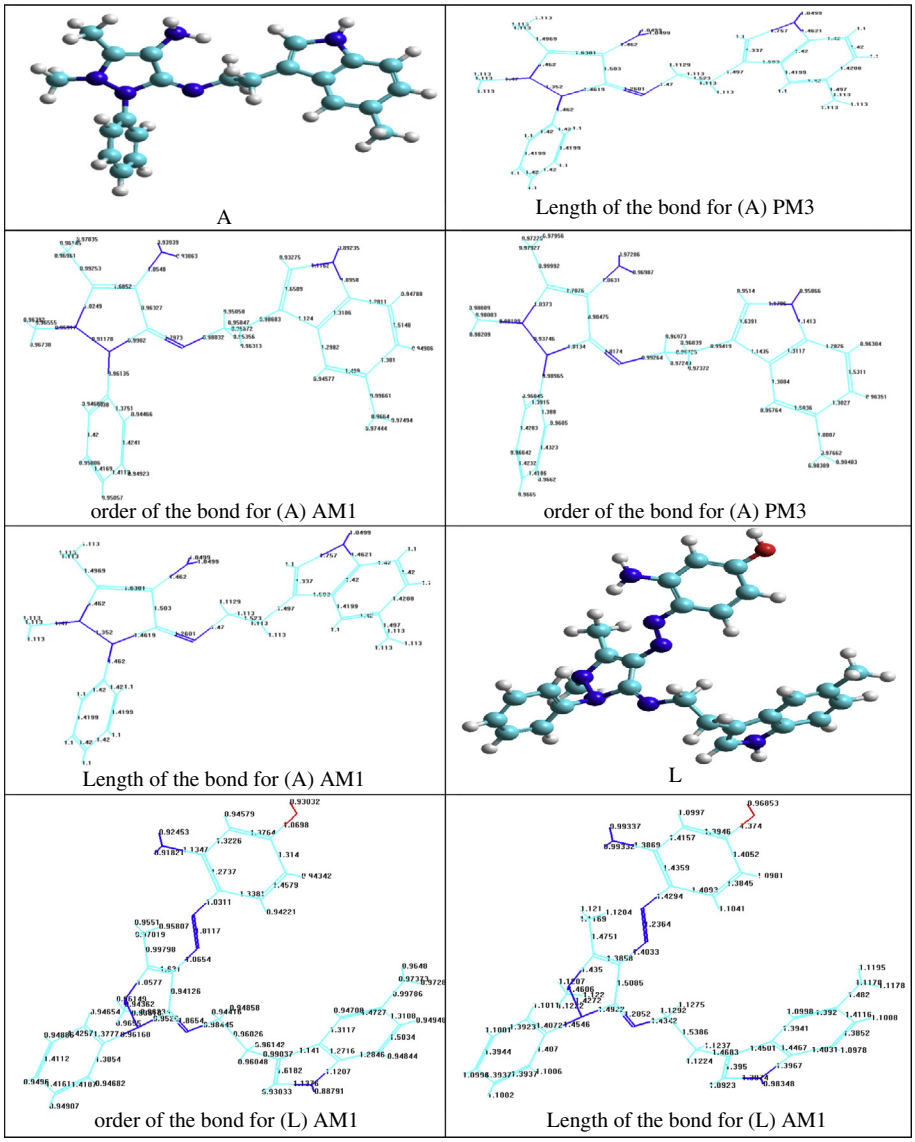

Fig. 3. conformation structure, bond length of A, ligand and complexes.

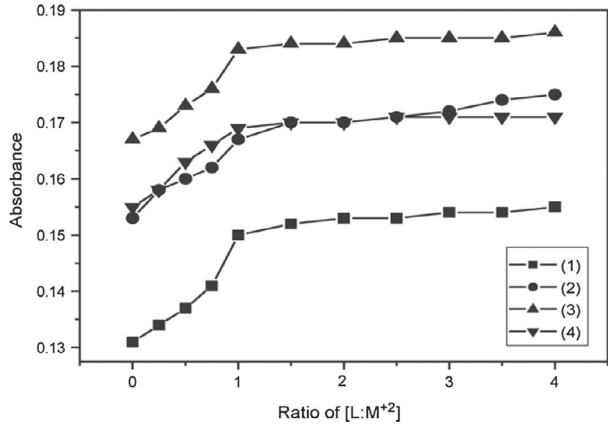

1-$[ZnL_2Cl]Cl$, 2-$[CdL_2Cl]Cl$, 3-$[NiL_2(H_2O)_2Cl]Cl$,4-$[PdL_2Cl]Cl$

Thermal analysis

The results of thermo gravimetric analyses of L and metals complexes are given in Table 4. The thermograms have been carried out in the range of 25–700 °C at a heating rate of 10 °C/min in nitrogen atmosphere, they showed an agreement in weight loss between their results obtained from the thermal decomposition and the calculated values, which supports the results of elemental analysis and confirms the suggested formulae. Thus, the ligand L showed a common general behavior as the first step ($C_{28}H_{29}N_7O$) was loss of $C_6H_6N_3O$ moiety followed by the other parts of the ligand, the final step of the thermolysis reactions of the complexes was found to give the metal oxide (see Table 5).

(L)-$C_{28}H_{29}N_7O$ [102.156% Found (100.209% Cal)]
(32–165 °C) → C_5H_6 [13.802% Found (13.782% Cal)]
(165–383 °C) → $C_{17}H_{19}N_4^-$ [13.802% Found (13.782% Cal)](383–598 °C) → $C_6H_6N_3O$[30.260% Found (28.385%Cal)

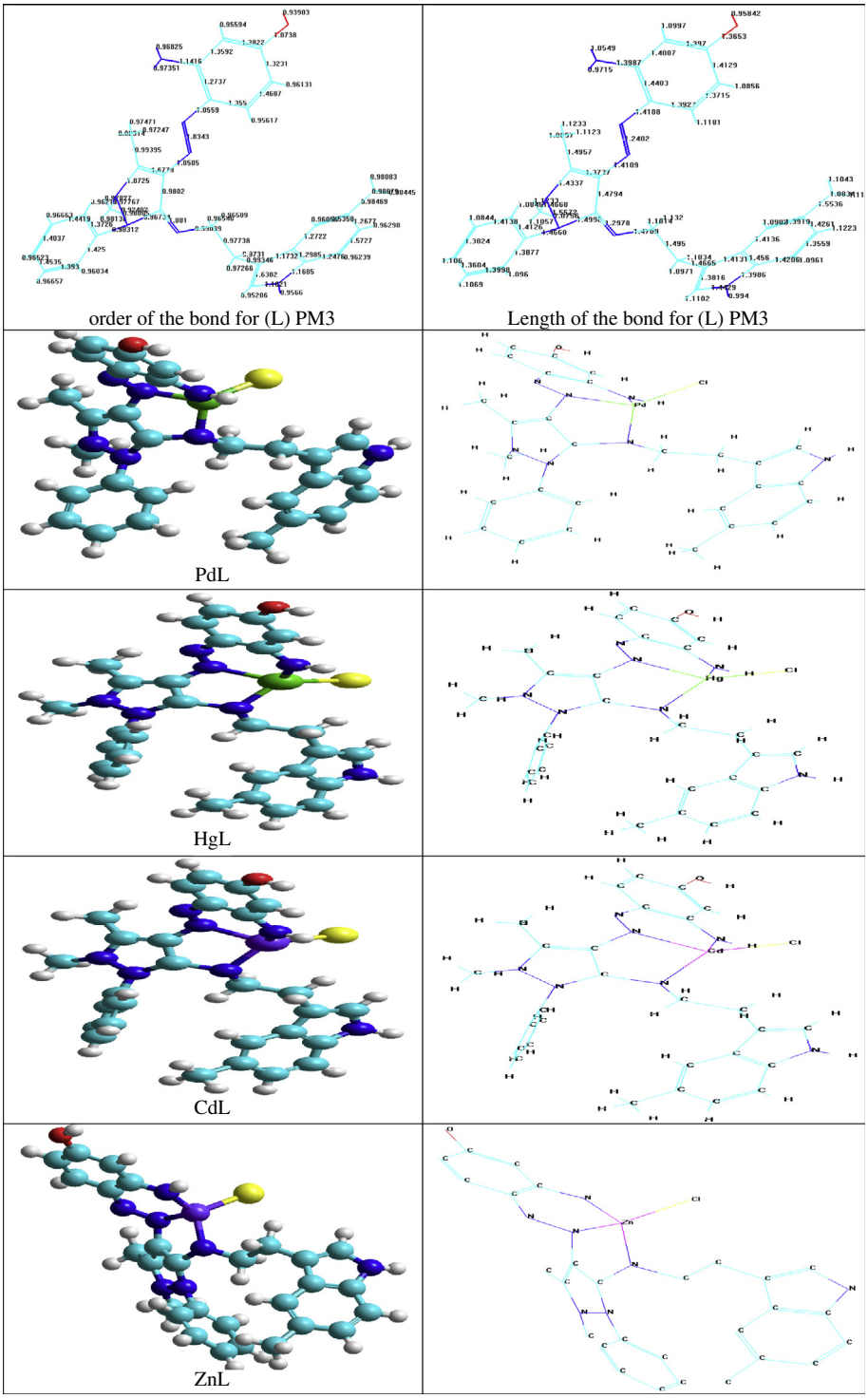

Fig. 3 (*continued*)

1-$C_{28}H_{29}N_7OCl_2Cd$ (662.89) (30–167 °C) → Cl + C_3H_8N [20.282% Found (19.459%Cal)]
2-$C_{25}H_{21}N_6OCd$ (533.896) (167–700 °C) → $C_{25}H_{21}N_6$ [61.015% Found (61.188%Cal)]
3-CdO [19.371% Found (19.352%Cal)]
Total wt. loos = 81.297% Found (80.647% Cal) and final residue: 18.703% Found (19.371% Cal)

1-$C_{28}H_{29}N_7OCl_2Pd$ (656.9) (25–210 °C) → C_2H_5 + Cl [15.223% Found (15.211%Cal)]
2-$C_{26}H_{24}N_7OPd$ (556.976) (210–430 °C) → $C_5H_{13}N_5$ [22.398% Found (21.822%Cal)]
3-$C_{21}H_{11}N_2OPd$ (413.626) (430–698 °C) → $C_{21}H_{11}N_2$ [44.824% Found (44.349%Cal)]

(*continued on next page*)

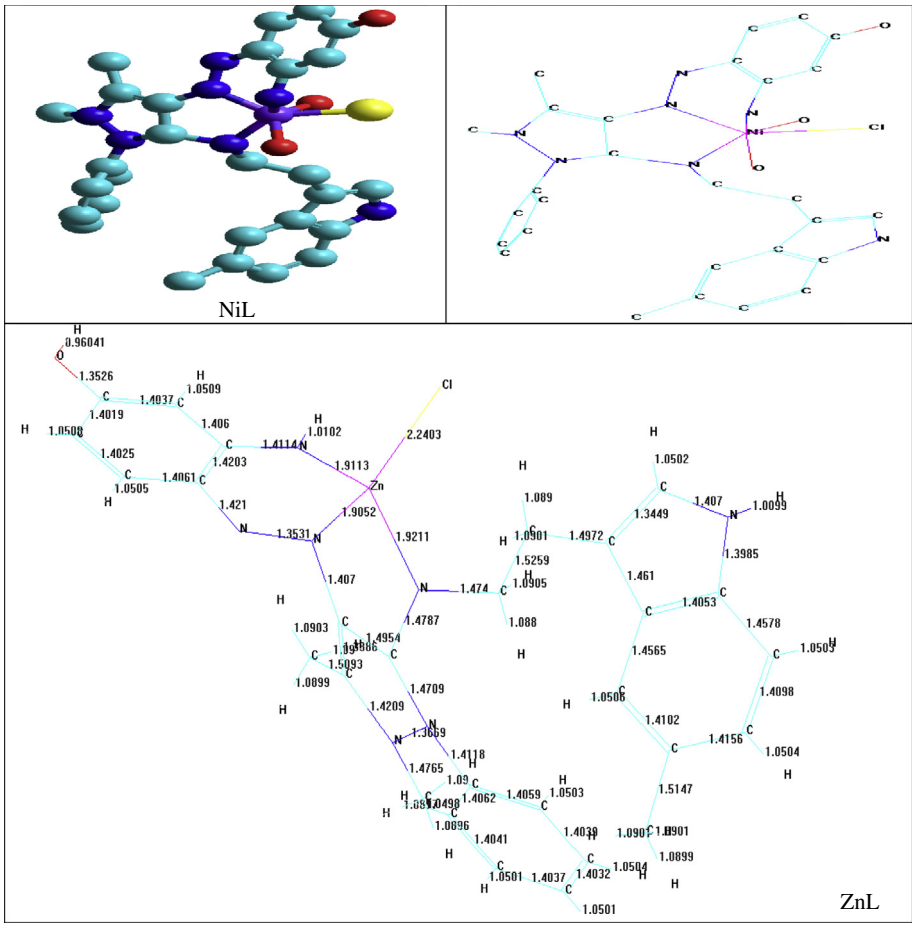

Fig. 3 (*continued*)

3-PdO [18.632% Found (17.555%Cal)]
Total wt. loos = 82.445% Found (81.382% Cal) and final residue: 18.618% Found (18.632% Cal)

1-$C_{28}H_{33}N_7O_3Cl_2Ni$ (645.21) (30–158 °C) → $2H_2O$ [6.127% Found (5.579%Cal)]
2-$C_{28}H_{29}N_7OCl_2Ni$ (609.21) (158–420 °C) → $C_4H_{10}NCl_2$ [21.601% Found (22.163% Cal)]
3-$C_{24}H_{19}N_6ONi$ (466.206) (420–700 °C) → $C_{24}H_{19}N_6$ [60.994% Found (60.693% Cal)
4-NiO [11.577% Found (11.564% Cal)]
Total wt. loos = 88.722% Found (88.435% Cal) and final residue:11.278% Found (11.577% Cal)

1-$C_{28}H_{29}N_7OCl_2Hg$ (751.1) (25–125 °C) → Cl [5.271% Found (4.720%Cal)]
2-$C_{28}H_{29}N_7OClHg$ (715.648) (125–430 °C) → C_7H_7NCl [22.821% Found (22.460%Cal)]
3-$C_{21}H_{22}N_4OHg$ (546.946) (430–698 °C) → $C_{21}H_{22}N_4$ [43.072% Found (43.995%Cal)]
4-HgO [28.836% Found (28.825%Cal)]
Total wt. loos = 71.164% Found (71.175% Cal) and final residue: 28.836% Found (28.836% Cal)

1-$C_{28}H_{29}N_7OCl_2Zn$ (615.9) (25–148 °C) → Cl + NH_2 [7.647% Found (8.363%Cal)]
2-$C_{28}H_{27}N_6OClZn$ (564.388) (148–425 °C) → $C_{10}H_{14}N_2Cl$ [31.601% Found (32.094%Cal)]
3-$C_{18}H_{13}N_4OZn$ (366.716) (425–695 °C) → $C_{18}H_{13}N_4$ [46.310% Found (46.341%Cal)]
4-ZnO [13.211% Found (13.202%Cal)]
Total wt. loos = 85.558% Found (86.798% Cal) and final residue: 14.442% Found (13.211% Cal)

1-$C_{28}H_{29}N_7OCl_4Pt$ (816) (30–132 °C) → Cl [5.271% Found (4.342%Cal)]
2-$C_{28}H_{29}N_7OCl_3Pt$ (781.048) (132–430 °C) → $C_3H_8Cl_3N$ [22.821% Found (22.842%Cal)]
3-$C_{25}H_{21}N_6OPt$ (594.542) (430–700 °C) → $C_{25}H_{21}N_6$ [50.096% Found (49.676%Cal)]
4-ptO [25.852% Found (23.139%Cal)]
Total wt. loos = 78.188% Found (76.860% Cal) and final residue: 21.812% Found (25.852% Cal)

Microbiological investigation

The biological activity of L ligand and its complexes were tested against bacteria; we used more than one test organism to increase the chance of detecting antibiotic principles in tested materials. The organisms used in the present investigation included two Gram positive bacteria (*B. subtilis* and *S. aureus*) and two Gram negative bacteria (*E. coli* and *P.* aeruginosa). The results of the bactericidal screening of the synthesized compounds are recorded in

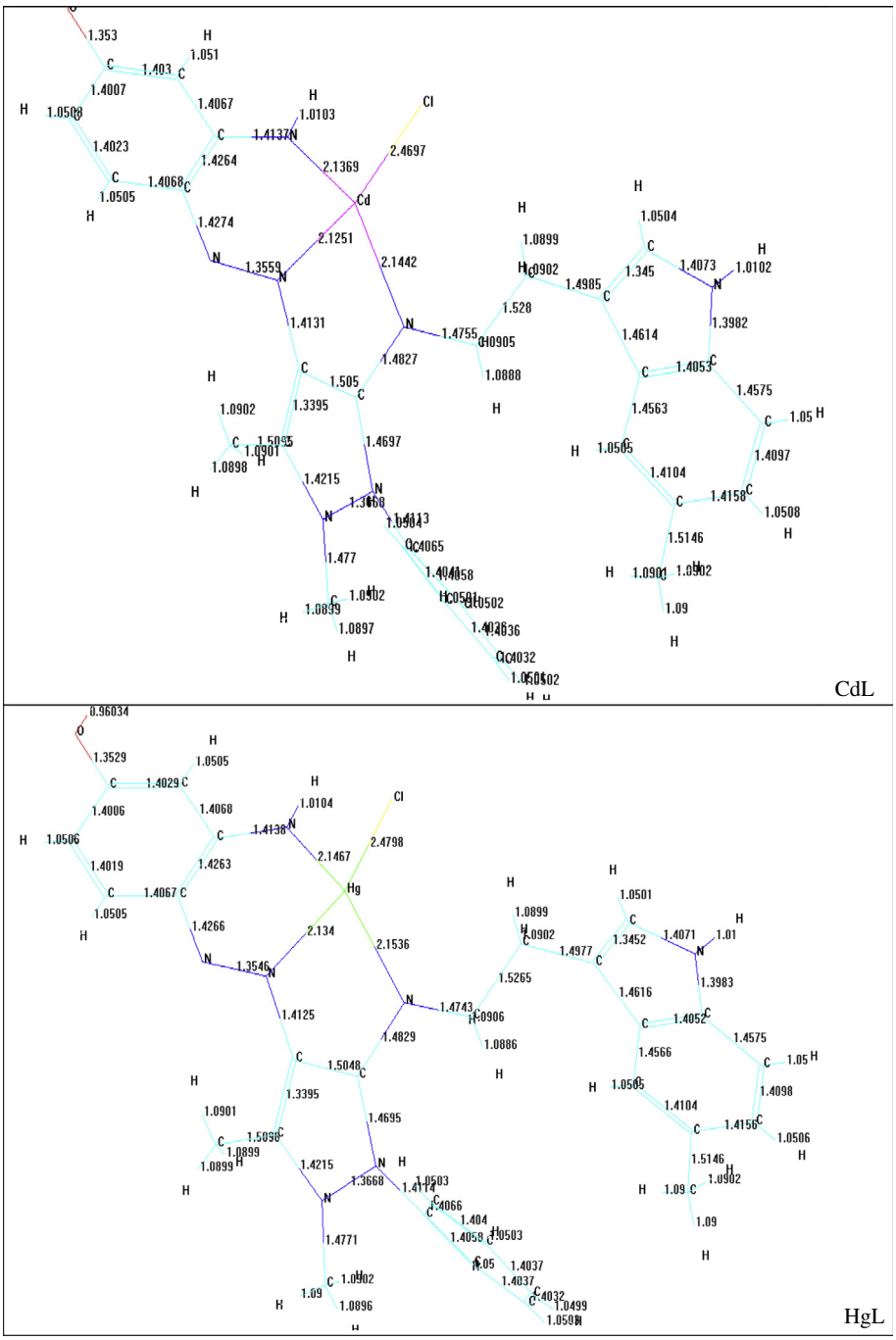

Fig. 3 (*continued*)

Table 6. An influence of the central ion of the complexes in the antibacterial activity against the tested Gram positive and Gram negative organisms show that the complexes have an enhanced activity compared to the ligand itself.

Theoretical study

The vibration spectra of the A and Azo-schiff base L were calculated by using a semi-empirical (PM3 and AM1) method. The results obtained for wave numbers are presented in Table 7, Fig. 1 and the comparison with the experimental values indicates some deviations. These deviations may be due to the harmonic oscillator approximation and lack of electron correlation. It was reported [29] that frequencies coupled with Hartree–Fock Theory (HFT) approximation and a quantum harmonic oscillator approximation tends to be 10% too high.

Electrostatic potential (E.P)

Electron distribution governs the electrostatic potential of molecules and describes the interaction of energy of the molecular system with a positive point charge, so it is useful for finding sites of reaction in a molecular positive charged species tend to attack a molecule where the E.P. is strongly negative electrophilic attach. The E.P of free ligands ware calculated and plotted as 2D contour to investigate the reactive sites of the molecules, and one can interpret the stereochemistry and rates of many reactive involving soft

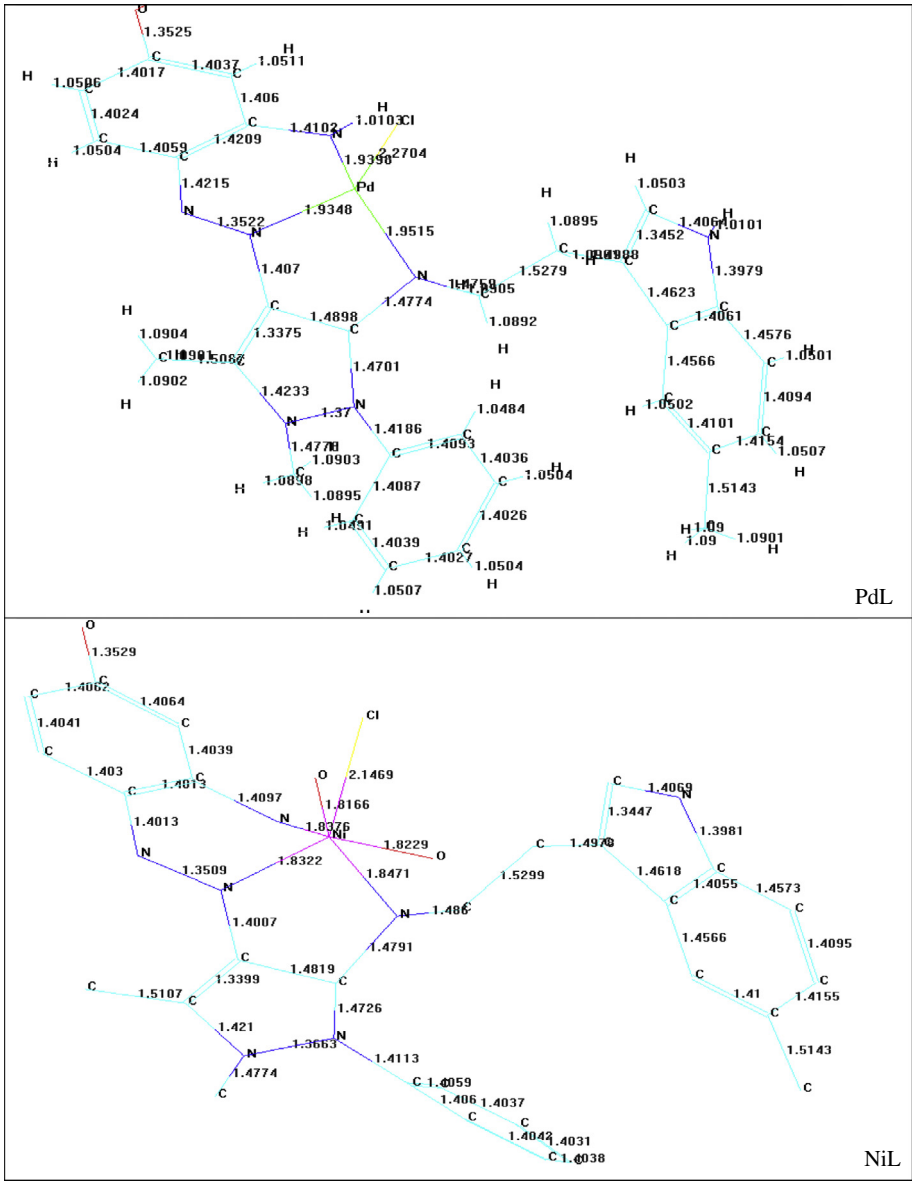

Fig. 3 (*continued*)

electrophiles and nucleophiles in terms of the properties of frontier orbitals (HOMO and LUMO). Overlap between the HOMO and LUMO values were plotted as 2D contour to get more information about these molecules Fig. 2. The results of calculation showed that the LUMO of transition metal ion prefers to react with the HOMO of nitrogen atoms of Azo-Schiff base ligand.

Optimized geometries energy of compounds

A theoretically probable structures of A metal complexes with Azo Schiff base were calculated to search for the most probable model building stable structure, these shapes, show the calculated optima geometries for A and Azo-schiff base L. The results of PM3 and AM1 method of calculation in gas phase for the binding energies and heat of formation of complexes are described in Table 8. Show the conformation structure, bond length of A, ligand and complexes Fig. 3.

Conclusion

In this paper we have explored the synthesis and coordination chemistry of some monomeric complexes obtained from the reaction of the tridentate ligand L with some metal ions. The mode of bonding and overall structure of the complexes were determined through physico-chemical and spectroscopic methods. Complexes formation study via molar ratio has been investigated and results were consistent to those found in the solid complexes with a ratio of (M:L) as (1:1). The thermodynamic parameters, such as ΔE^*, ΔH^*, ΔS^* ΔG^* and K are calculated from the TGA curve using Coats–Redfern method. Hyper Chem-8 program was used to predict structural geometries of compounds in gas phase. The heat of formation (ΔHf°) and binding energy (ΔEb) at 298 K for the A, free ligand and its complexes was calculated by PM3 method. The synthesized ligand and its metal complexes were screened for their biological activity against bacterial species, two Gram positive

bacteria (*B. subtilis* and *S. aureus*) and two Gram negative bacteria (*E. coli* and *P.* aeruginosa.

References

[1] Y. Wang, Y. Liu, J. Luo, H. Qi, X. Li, M. Nin, M. Liu, D. Shi, W. Zhu, Y. Cao, Metallomesogens based on platinum(II) complexes: synthesis, luminescence and polarized emission, Dalton Trans. 40 (2011) 5046–5051.

[2] N.C. Oforka, V.N. Mkpenie, A new method of synthesis of azo Schiff base ligands with azo and azomethine donors: Synthesis of *N*-4-methoxy-benzylidene-2-(3-hydroxyphenylazo)-5-hydroxyaniline and its nickel(II) complex, Chin. J. Chem. 25 (2007) 869–871.

[3] S.N. Pandeya, D. Sriram, G. Nath, E. de Clercq, Synthesis and pharmacological evaluations of some novel isatin derivatives for antimicrobial activity, Il Farmaco. 54 (1999) 624–628.

[4] M. Lashanizadegan, M. Jamshidbeigi, Synthesis of N,N′-bis[4 (benzeneazo) salicylaldehyde]4-methyl-1,2-phenylenediamine and its transition metal complexes., Synth. React. Inorg. Metal-Org. Nano-Metal Chem. 42 (2012) 507–512.

[5] E.M. Hodnett, W.J. Dunn, Synthesis of novel azo Schiff base bis [5-(4-methoxyphenylazo)-2-hydroxy-3-methoxy benzaldehyde]-1,2-phenylene diimine, J. Med. Chem. 13 (1970) 768–770.

[6] S.B. Desai, P.B. Desai, K.R. Desai, Synthesis and spectroscopic studies of new Schiff bases, Hetrocycl. Commun. 7 (2001) 83–90.

[7] L. Mitu, M. Ilis, N. Raman, M. Imran, S. Ravichandran, Transition metal complexes of isonicotinoyl-hydrazone-4-diphenylaminobenzaldehyde: synthesis, characterization and antimicrobial studies., EJ. Chem. 9 (2012) 365–372.

[8] S. Samadhiya, A. Halve, 1-(4-{[(*E*)-(4-Diethylamino-2 hydroxyphenyl) methylene]amino} phenyl)ethanone, Orient. J. Chem. 17 (2001) 119–122.

[9] Z. Rezvani, L. Ahar, K. Nejati, S.M. Seyedahmadian, Synthesis, characterization and liquid crystalline properties of new bis[5-((4-alkoxyphenylazo) *N*-(alkyl)-salicylal deminato]coppe(II) and Nickel(II) complexes homologues, Acta Chim. Slov. 51 (2004) 675–686.

[10] S. Cakir, E. Bicer, M. Odabasoghu, C.J. Albayrak, A new method of synthesis of azo Schiff base ligands with azo and azomethine donors: synthesis of N-4-methoxy-benzylidene-2-(3-hydroxyphenylazo)-5-hydroxy-aniline and its Nickel(II) complex, Braz. Chem. Soc. 16 (2005) 711–715.

[11] P. Bhattacharyya, J. Parr, A.T. Ross, First synthesis of a unique dilead Schiff base complex, Dalton Trans. 1998 (1998) 3149–3150.

[12] H. Nazir, H. Nazir, N. Sapmaz Akben, M. Bürke Ateş, H. Sözeri, I. Ercan, O. Atakol, F. Ercan, Synthesis, crystal structure and magnetic behaviourof a mononuclear Fe(III)-Schiff base metal complex, Z. Kristallogr. 221 (2006) 276–289.

[13] N.N. Das, A.C. Dash, Synthesis, characterization and electrochemistry of a binuclear copper(II) complex of Schiff base derived from 2-aminomethyl benzimidazole and salicylaldehyde, Polyhedron., 1995, 14, 1221–1227. Molecules 2012, 17 6446.

[14] A. Khandar, K. Nejati, Synthesis and characterization of cyano-bridged polynuclear $[Cu(dmpn)_2]3[Co(CN)_6]_2{\cdot}12H_2O$ and trinuclear $[Cu(dmpn)_2]2[Co(CN)_6]ClO_4{\cdot}3H_2O$ complexes, Polyhedron 19 (2000) 607–613.

[15] A.A. Khandar, Z. Rezvani, K. Nejati, I. Yanovsky, J.M. Martines, Synthesis, characterization and liquid crystalline properties of new bis[5-((4-alkoxyphenylazo)-*N*-(alkyl)-salicylaldeminato] Nickel(II) complexes, Acta Chim. Slov. 49 (733) (2002) 741.

[16] A.A. Khandar, K. Nejati, Z. Rezvani, Syntheses, characterization and study of the use of Cobalt (II) Schiff-base complexes as catalysts for the oxidation of styrene by molecular oxygen, Molecules 10 (2005) 302–311.

[17] L. Nejati, Z. Rezvani, Syntheses, characterization and mesomorphic properties of new bis(alkoxyphenylazo)-substituted N,N′ salicylidene diiminato Ni(II), Cu(II) and VO(IV) complexes, New J. Chem. 27 (2003) 1665–1669.

[18] H.A. Dorestt, A review of quantum chemical studies of energetic materials, 1996. DSTO Technical report.

[19] J.C. Foresman, C. Frisch, Exploring Chemistry with Electronic Structure Methods, second ed., Gaussian Inc., 1996.

[20] A.W. Coats, J.P. Redfern, Kinetic parameters from thermogravimetric, Nature 201 (1964) 68.

[21] H.H. Horovitz, G. Metzger, Analysis of thermogravimetric traces as an approach to determine the mechanism of dissociation of copper (II)-α-aryl azo acetoacetyl aminopyridine chelates, Thermochim. Acta 159 (1963) 43–54.

[22] Abbas A.S. Al-Hamdani, Shayma A. Shaker, Synthesis, Characterization, structural studies and biological activity of a new Schiff Base-Azo ligand and its complexation with selected metal ions, J. Oriental Chem. 27 (2011) 835–845.

[23] Wail Al Zoubi, F. Kandil, M.K. Chebani, Synthesis of N2O2S2-Schiff bases and using them to transport Cu2+ by bulk liquid Membrane., Int. J. ChemTech Res. USA 3 (2011) 1612–1621.

[24] K. Nakamoto, Infrared and Raman Spectra of Inorganic and Coordination Compounds, Wiley-Inter Science, New York, 1997.

[25] R.M. Silverstein, G.C. Bassler, T.C. Movril, Spectroscopic Identification of Organic Compounds, fouth ed., Wiley, New York, 1981.

[26] A.S. Shaymab, E-J. Chem. 8 (2011) 153–158.

[27] A.B.P. Lever, Inorganic Electronic Spectroscopy, Elsevier, New York, 1968. NY, USA.

[28] A. Golcu, M. Tumer, H. Demirelli, R.A. Wheatley, Inorg. Chim. Acta (2000) 358.

[29] B.M. Chamberlain, Y. Sun, J.R. Hagadorn, E.W. Hemmesch, A.V. Hillmyer, W.B. Tolman, Macromolecules 32 (1999) 2400.